47. Tuffrau, M. 1960. Révision du genre *Euplotes*, fondée sur la comparaison des structures superficielles. *Hydrobiologia*, **15**:1–77.
48. Tuffrau, M. 1964. Le maintien des caractères spécifiques à travers le polymorphisme d'*Euplotes balteatus* Dujardin, 1841. *Arch. Zool. Exp. Gén.*, **104**:143–151.
49. Tukey, J. W. 1977. Exploratory Data Analysis. Addison-Wesley Publishing Company, Reading, Massachusetts. Pp. 506.
50. Valbonesi, A., Ortenzi, C. & Luporini, P. 1987. Observations on the biology of *Euplotes charon* (Hypotrichida, Ciliophora). *Boll. Zool.*, **54**:111–118.
51. Valbonesi, A., Ortenzi, C. & Luporini, P. 1988. An integrated study of the species problem in the Euplotes *crassus-minuta-vannus* group. *J. Protozool.*, **39**:45–54.
52. Valbonesi, A., Ortenzi, C. & Luporini, P. 1992. The species problem in a ciliate with a high multiple mating type system, *Euplotes crassus*. *J. Protozool.*, **204**:171–180.
53. Van Keulen, H., Gutell, R. R., Gates, M. A., Campbell, S. R., Erlandsen, S. L., Jarroll, E. L., Kulda, J. & Meyer, E. A. 1993. Unique phylogenetic position of Diplomonadida based on the complete small ribosomal RNA sequence of *Giardia ardeae, G. muris, G. duodenalis* and *Hexamita* sp. *FASEB J.*, **7**:223–231.
54. Wichterman, E. 1964. Descriptions and life cycle of *Euplotes neapolitanus* sp. nov. (Protozoa, Ciliophora, Hypotrichida) from the Gulf of Naples. *Trans. Amer. Microsc. Soc.*, **83**:362–370.

Received 5-10-93, 2-11-94; accepted 3-7-94

J. Euk. Microbiol., 41(5), 1994, pp. 450–457

Napamichum cellatum N. Sp. (Microspora, Thelohaniidae), a New Parasite of Midge Larvae of the Genus *Endochironomus* (Diptera, Chironomidae) in Sweden

EVA K. C. BYLÉN[1] and J. I. RONNY LARSSON
Department of Zoology, Helgonav. 3, University of Lund, S-223 62 Lund, Sweden

ABSTRACT. The new microsporidium, *Napamichum cellatum*, a parasite of the adipose tissue of midge larva of the genus *Endochironomus* in Sweden, is described based on light microscopic and ultrastructural characteristics. Plurinucleate plasmodia with nuclei arranged as diplokarya divide, probably by plasmotomy, producing a small number of diplokaryotic merozoites. The number of merogonial cycles is unknown. Each diplokaryotic sporont yields eight monokaryotic sporoblasts in a thin-walled, more or less fusiform sporophorous vesicle. A small number of multisporoblastic sporophorous vesicles were observed, in which a part of the sporoblasts were anomalous. The sporogony probably begins with a meiotic division. The mature spores are slightly pyriform. Fixed and stained spores measure 2.1–2.4 × 3.7–4.5 μm. The five-layered spore wall is of the *Napamichum* type. The polar filament is anisofilar with seven to eight coils (142–156 and 120 nm wide). The angle of tilt is 55–65°. The polaroplast has an anterior lamellar and a posterior tubular part. The granular, tubular and crystal-like inclusions of the episporontal space disappear more or less completely when the spores mature. The crystal-like inclusions are prominent in haematoxylin staining, but not visible with the Giemsa technique. The microsporidium is compared to other octosporoblastic microsporidia of midge larva and to the species of the genera *Chapmanium* and *Napamichum*.

Supplementary key words. Taxonomy, ultrastructure.

IN the autumn of 1986, a microsporidium with lightly pyriform octospores was found in the adipose tissue of a midge larva collected in southern Sweden. The sporulation took place in lightly fusiform sporophorous vesicles with prominent crystalline inclusions. The parasite was tentatively identified as the species which, at that time, was known as *Chapmanium dispersus* Larsson, 1984 [5]. When the microsporidium was studied using electron microscopy several years later, it became apparent that it was a different species, one that belongs to the genus *Napamichum* Larsson, 1990 [6].

The microsporidium, which is new to science, is briefly described herein. It is compared to species of the genera *Chapmanium* and *Napamichum* and to octosporoblastic microsporidia from midge larvae. The taxonomic considerations are discussed with special attention to ultrastructural features.

MATERIALS AND METHODS

The host was one of two specimens of an unidentified species of the genus *Endochironomus* Kieffer in a sample of midge larvae collected from a pond at Vikhög in the region of Scania, southern Sweden, on October 7, 1986. To our knowledge it is impossible to identify midge larvae to species without rearing to adult stage, and that was impossible in this case.

Permanent squash preparations were lightly air dried, fixed in Bouin-Duboscq-Brasil solution overnight (Picric acid from Merck, Darmstadt, FRG) and stained using Giemsa (Fluka AG, Buchs, FRG) solution or Heidenhain's iron haematoxylin (Merck).

For paraffin sectioning, a few segments of the body were fixed in the same fixative overnight, washed and dehydrated in an ascending series of ethanols, cleared in butanol and embedded in paraplast. Sections were cut sagittally at 10 μm and stained using Heidenhain's iron haematoxylin. For details on the histological techniques, see the manual by Romeis [8]. All permanent preparations were mounted in DePeX (BDH Chemicals Ltd., England). Measurements were made with an eye-piece micrometer at ×1,000.

For transmission electron microscopy, one piece of an infected segment was excised and fixed in 2.5% (v/v) glutaraldehyde (BDH Chemicals) in 0.2 M sodium cacodylate buffer (pH 7.2) at 4° C for 4 h. After washing in cacodylate buffer and postfixation in 2.0% (w/v) osmium tetroxide (Agar Scientific Ltd., UK) in cacodylate buffer for 1 h in 4° C, the piece was washed and dehydrated in an ascending series of buffer-acetone solutions, to absolute acetone, and embedded in Epon. Sections were stained using uranyl acetate and lead citrate [7].

[1] To whom correspondence should be addressed.

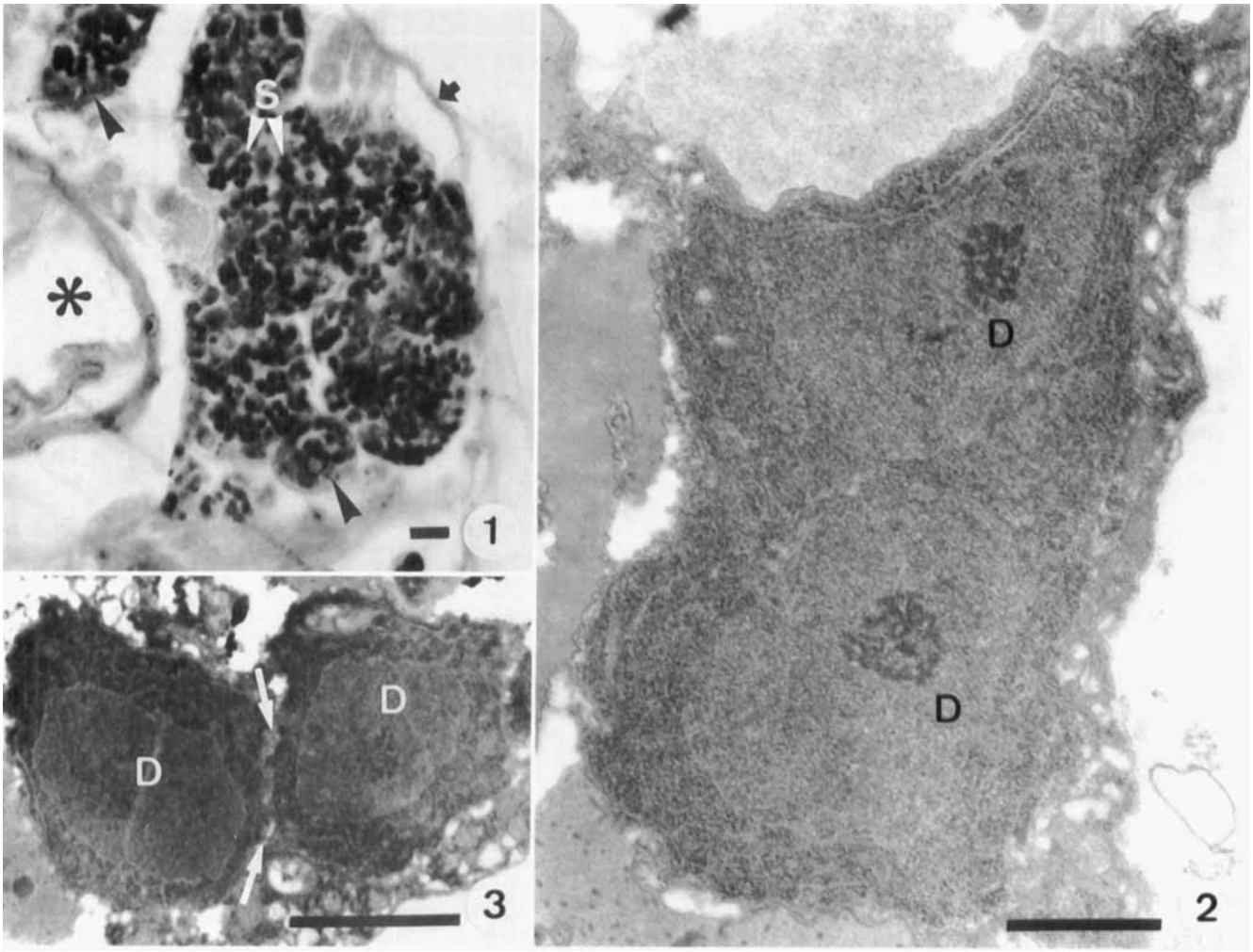

Fig. 1–3. Pathogenicity and life cycle of *Napamichum cellatum* n. sp. **1**. Semithin sagittal section of an infected midge larva, Heidenhain's haematoxylin. The fat body cells are filled with more or less fusiform sporophorous vesicles (S) with mature spores, and a small number of presporal stages (arrow heads). Bar = 10 μm. Asterisk, gut lumen; arrow, hypoderm. **2**. Electron micrograph of a merogonial plasmodium with two diplokarya (D) visible. Bar = 1 μm. **3**. Electron micrograph of two partly connected diplokaryotic (D) merozoites (M). The plane of the division is indicated by arrows. Bar = 2 μm.

RESULTS

Pathogenicity and prevalence. One of two larvae of the same species was infected. Midge larvae of other species had no microsporidia.

The whitish adipose tissue was shining through the hypoderm, indicating a heavy infection, but the sections revealed that at least ¼ of the fat body of this specimen was unaffected. The unaffected parts of the fat body were situated on the ventral side of the larva and close to the gut. The infected fat body was slightly hypertrophic. No syncytium was formed (Fig. 1).

Merogony. The earliest stages observed were merogonial plasmodia. Their cell wall is a plasma membrane, about 8 nm thick without external reinforcements, and the nuclei are coupled as diplokarya (Fig. 2, 4). Groups of 8–15 merozoites, with a few of the merozoites still partly associated, were observed. This might imply that the plasmodia divide by plasmotomy (Fig. 3). Rosette-like budding was not observed. It is unknown if there is more than one sequence of merogony.

Fixed and stained merozoites measure 2.8–3.7 μm in diameter. The central diplokaryon measures 1.6–2.6 μm in diameter. The cytoplasm is electron dense, with numerous free ribosomes, and it is traversed by strands of the endoplasmic reticulum (Fig. 3).

Sporogony. The last, or possibly only, generation of merozoites matures to sporonts (Fig. 5, 6). The two components of the diplokaryon separate, and probably divide reductionally (Fig. 7). Rosette-like budding yields initially lobed plasmodia with four isolated nuclei (Fig. 8, 14) and, after a subsequent mitosis, 8-lobed plasmodia with isolated nuclei (Fig. 9). Sporoblasts are budded off simultaneously (Fig. 10, 11). Anomalous sporogony resulting in multisporoblastic sporophorous vesicles, where a part of the sporoblasts were anomalous, was observed. It seems to occur rarely.

In ultrathin sections the beginning of the sporogony is revealed by electron-dense material being secreted outside the plasma membrane of the sporont, and by an internal reorganization resulting in less electron-dense cytoplasm. The dense material yields the wall of a sporophorous vesicle, which is initiated as blisters on the surface of the sporont. Inside the blisters, continued secretion of electron-dense material yields the thick sporont wall (Fig. 12). Excess wall material projects into the episporontal space. When the plasmodium has reached the lobed stage, the excess wall material appears as a reticulum

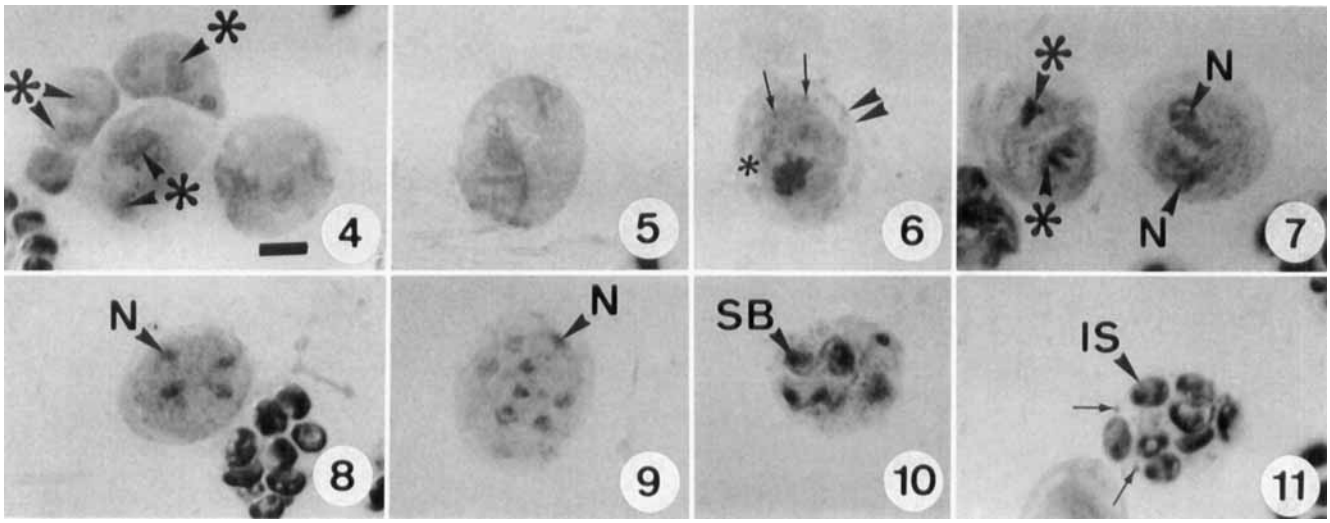

Fig. 4–11. Light micrographs of developmental stages; Heidenhain's haematoxylin. Bar = 5 μm. **4.** Dividing diplokaryotic (asterisks) merogonial plasmodia. **5.** An early sporont; the two components of the diplokaryon have separated. **6.** A later sporont. The sporophorous vesicle (arrow heads) is visible; crystal-like inclusions (arrows) are present in the episporontal space (asterisk). **7.** Two sporonts with dividing nuclei (N), the chromatin (asterisks) is visible. **8.** A sporont at the four nuclei stage (N, nucleus). **9.** A sporont at the eight nuclei stage. **10.** A sporont in the process of budding off sporoblasts (SB). **11.** A sporophorous vesicle with eight immature spores (IS); crystal-like inclusions are visible (arrows).

or a honey-comb-like layer connected with the lobes of the plasmodium (Fig. 13).

The mature spore. The mature spores are slightly pyriform and measure 2.1–2.4 × 3.7–4.5 μm (n = 19), in fixed and stained squash preparations (Fig. 15, 16).

The spore wall is of normal construction for the genus *Napamichum*: a plasma membrane approximately 6 nm thick, an electron-lucent endospore that measures 45–54 nm at the anterior pole and 112–180 nm over the rest of the spore, and outermost, a complex, 50–57-nm-thick, five-layered exospore. From the inside proceeding outward, the following subdivisions are visible: a thin strand of electron-dense material delimits an electron-dense, ca. 20-nm-thick layer towards the endospore; followed by a 2–3-nm-thick, electron-dense strand; an 8–10-nm, moderately dense layer; a ca. 5-nm double layer and finally, a moderately electron-dense layer, ca. 18 nm thick, with an indistinct external border (Fig. 17, 18).

The polar filament is of the anisofilar type, ca. 180 nm wide where it attaches to the anchoring disc at the anterior pole of the spore. The diameter tapers to the point where it curls up to form seven to eight coils in the posterior part of the spore. The angle of tilt of the first filament coil to the long axis of the spore is 55–65°. The first four to five coils have the largest diameter, measuring 142–156 nm. The three to four following coils are more narrow, ca. 120 nm. The transversely cut filament exhibits five concentric layers of varying electron density, which are, in inward direction: 1. a ca. 6-nm-thick unit membrane; 2. a ca. 7-nm, moderately electron-dense layer; 3. a prominent, 8–9-nm-wide electron dense layer; 4. a moderately dense layer, 28–36 nm, with a fringe of more or less longitudinally directed fibrils, and 5. a 42–50-nm-wide core, that exhibits electron-dense concentrical bands (Fig. 17, 19). The anchoring disc at the anterior pole of the spore is of normally layered construction.

The umbrella-like polar sac encloses about ⅔ of the anterior polaroplast (Fig. 17). The polaroplast consists of two parts in which the compartments are lined with approximately 6-nm-thick unit membranes. In the anterior polaroplast, which measures about ¼ of the spore length, the compartments are about 15-nm-wide lamellae, arranged in concentric layers around the straight portion of the polar filament. The distance between the lamellae narrows from ca. 30 nm anteriorly to ca. 15 nm in the posterior part of the anterior polaroplast. The posterior polaroplast surrounds the bent section of the filament and ends at the level of the first filament coil. The nucleus is situated on this level as well. The compartments are tubular, measuring 135–158 nm in diameter (Fig. 17).

The single nucleus appeared bent, and it was difficult to measure. Ultrathinly sectioned nuclei measured 0.7–0.9 μm in diameter (Fig. 17).

The cytoplasm is moderately electron dense, with prominent strands of polyribosomes, especially around the nucleus and close to the filament coils (Fig. 17). The posterior vacuole is 1.0–1.1 μm wide. It was never well fixed (Fig. 17).

The sporophorous vesicle. The sectioned, and hence not compressed, sporophorous vesicles are more or less fusiform (Fig. 1), but squashed vesicles usually appear ovoid. They measure 11.7–14.3 × 13.8–17 μm when containing mature spores (Fig. 16). The wall is ca. 6 nm thick (Fig. 18, 20, 23). Three types of inclusions are observed in the episporontal space. A moderately electron-dense, finely granular material appears when the vesicle is initiated. It gradually disintegrates during sporogony and most of it has disappeared by the time the spores are mature (Fig. 14, 17). Crystal-like and reticulate inclusions appear when the sporont wall begins to develop (Fig. 12, 20, 21). They are made of excess sporont wall material. The crystals measure 220–370 nm in diameter and look like large electron-dense rounded bodies which contain internal droplets of less electron-dense material. Crystals are formed in great numbers, and they are easily observed in preparations stained with haematoxylin, but almost invisible in Giemsa stained preparations. Only a small number remain in vesicles with mature spores (Fig. 6, 11, 12, 14, 16, 17, 21). The tubular inclusions look different depending on the stage of the sporogony that yields the excess wall material. The tubular inclusions produced last are 35–55 nm wide, and they resemble sporoblast wall material (Fig. 14, 22). Tubules of a more delicate construction, 32–60 nm wide, were observed in

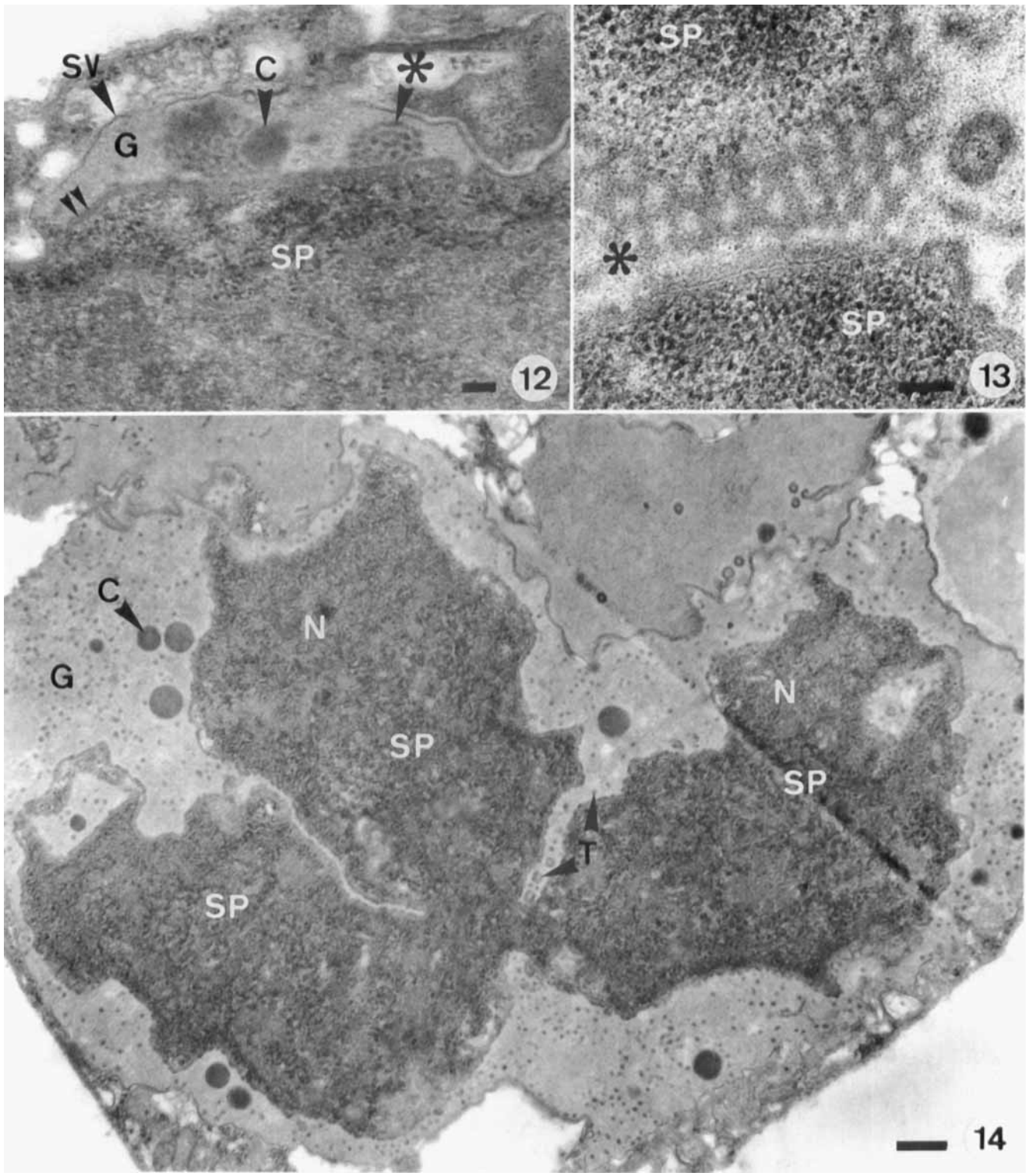

Fig. 12–14. Electron micrographs of the sporogony of *Napamichum cellatum* n. sp. **12**. The sporophorous vesicle (SV) is initiated as blisters outside the sporont (SP). The electron dense material excreted from the sporont produces the sporont wall (arrow heads), and excess material forms the granular (G), reticulate (*), and the crystal-like (C) inclusions of the episporontal space. Bar = 100 nm. **13**. The reticulate material forms a honeycomb-like layer (*) between the lobes of the sporont (SP). Bar = 100 nm. **14**. Rosette-like division of a sporont at the four nuclei stage, with two nuclei (N) and three lobes (SP) visible inside the sporophorous vesicle. The episporontal space contains large amounts of granular (G) inclusions and scattered crystal-like (C) inclusions; tubular (T) inclusions appear at the base of the lobes. Bar = 0.5 μm.

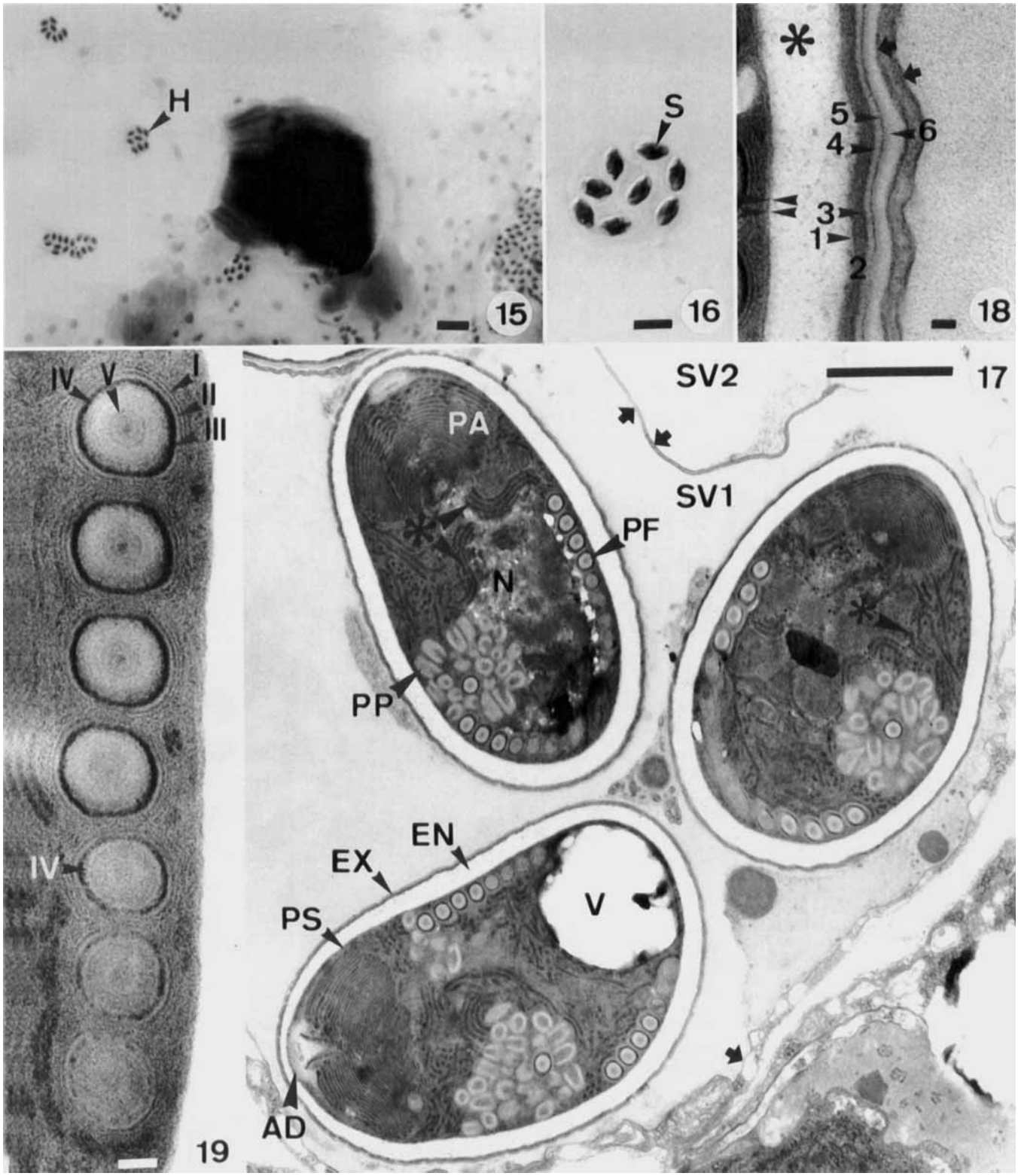

Fig. **15–19**. Mature spores of *Napamichum cellatum* n. sp. **15**. Light micrograph of slide no. 861007-C-4 with the holotype (H) indicated. Bar = 15 μm. **16**. Light micrograph of a sporophorous vesicle with eight mature spores (S); note the absence of inclusions in the episporontal space. Bar = 5 μm. **17**. Electron micrograph of mature spores inside a sporophorous vesicle (SV 1). A second sporophorous vesicle (SV 2) is bordering (arrows indicate the envelopes). Note the reduced amount of inclusions in the episporontal space. In the spores the anchoring disc (AD), the polar sac (PS), the anterior part of the polaroplast (PA), the posterior part of the polaroplast (PP), the polar filament (PF), the nucleus (N), the posterior vacuole (V), the lucent endospore (EN), the layered exospore (EX), and the polyribosomes (*) are visible. Bar = 1 μm. **18**. Electron micrograph of the spore wall at greater magnification: plasma membrane (arrow heads), the lucent endospore (*) and the layered exospore where no. 1 indicates

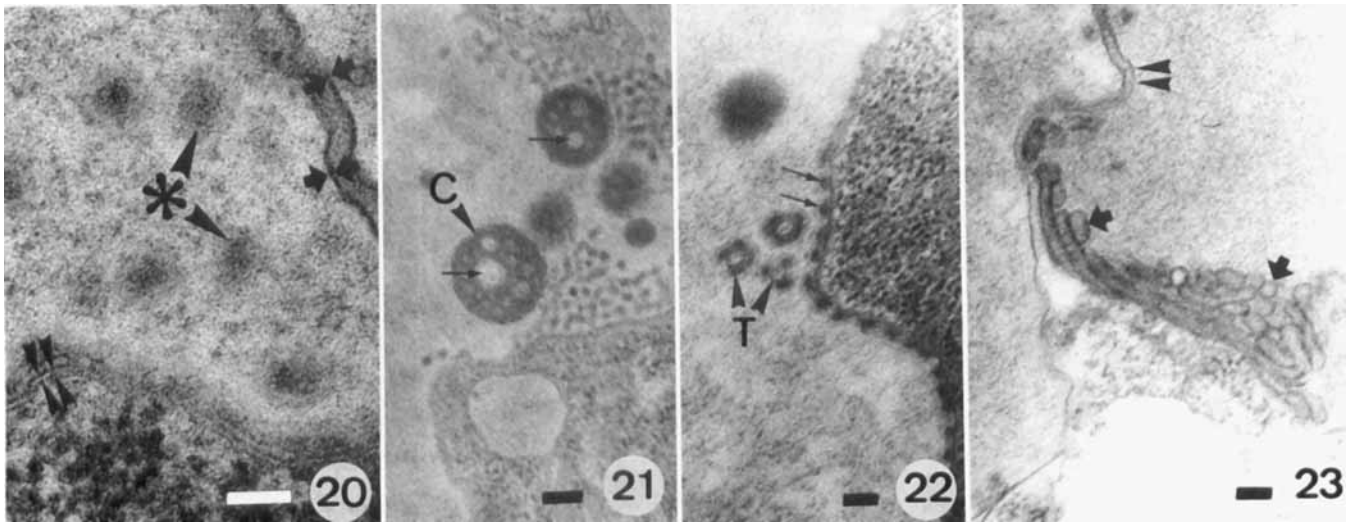

Fig. 20–23. Electron micrographs of the inclusions of the episporontal space. **20**. Rounded electron-dense material (*), of the same texture as the dense sporont wall, that later forms the reticulate inclusions (arrowheads indicate the plasma membrane, arrows the envelope of the sporophorous vesicles); the two vesicles visible are only separated by a narrow strand of host cytoplasm). **21**. Crystal-like inclusions (C) composed of material of two densities (arrows) appear approximately simultaneously with the rounded inclusions. **22**. When sporoblast-lobes are formed, layered exospore-material gives rise to tubular inclusions (T). Note the regular patches of exospore material (arrows) visible both on the sporoblast-lobes and in the walls of the tubules. **23**. Two adjacent sporophorous vesicles (arrowheads indicate the envelope); envelope folds give the impression of closely associated thin-walled tubules (arrows). Scale bars = 100 nm.

close connection with the sporophorous vesicle. When transversely sectioned, their walls resemble the thin wall of the sporophorous vesicle (Fig. 23), and we interpret them as folds of the vesicle.

DISCUSSION

Numerous microsporidian species are parasites of the fat body of midge larvae. If we disregard the species whose spore shapes and sporogony are clearly different from the species described herein, five named and three unnamed species remain. These eight species produce oval to pyriform spores in octosporous sporophorous vesicles and are presented in Table 1 as: *Amblyospora macrococcus* (Voronin, 1979) [9, 10], *Amblyospora* sp. Voronin, 1991 [10], *Amblyospora* sp. Garcia & Lange, 1986 [1], *Napamichum dispersus* (Larsson, 1984) [5], *Thelohania breindli* Weiser, 1946 [11], *T. corynoneurae* Voronin, 1979 [9], *T. pinguis* Hesse, 1903 [2], and *Thelohania* sp. Hilsenhoff & Lovett, 1966 [3]. The three *Amblyospora* species produce the barrel-shaped spores characteristic of their genus, and they also have the characteristic complex *Amblyospora*-exospore. The ultrastructural cytology of the *Thelohania* species is completely unknown, so only a few discriminating characters are available for comparison. However, the spores of *T. corynoneurae* are distinctly larger, and the spores of *T. breindli* distinctly smaller than the spores of the species described herein. If the spore sizes of the unnamed *Thelohania* species and of *T. pinguis* refer to fixed spores, these spores approach the inferior limit of the spores of the Swedish microsporidium. However, these species are also clearly different. The sporophorous vesicles of *T. pinguis* are approximately only half as large as the vesicles of the species described herein, and if we extend the comparison to include the pathological effects, both species can be excluded. Both of them distort the infected fat body cells and generate voluminous tumor-like masses, clearly different from the pathological effects seen in the Swedish material. The remaining species, *N. dispersus*, has distinctly wider and slightly longer spores, and also ultrastructural differences (the number of polar filament coils, the internal difference between wide and narrow coils, and the arrangement of the compartments of the polaroplast).

The shape of the spores and the sporophorous vesicles suggests two possible genera for this microsporidium: *Chapmanium* Hazard & Oldacre, 1975 [4] and *Napamichum* Larsson, 1990 [6]. The latter genus was established after a comparison with *Chapmanium cirritus* Hazard & Oldacre, 1975, the type species of the genus, where upon it was seen that the thick, complex exospore of the genus *Napamichum* is absent from *C. cirritus*. This type of exospore is present in the species described herein, which indicates that it belongs in *Napamichum*.

This genus also comprises a second species, *N. aequifilum* Larsson, 1960 [6]. This species has spores of similar size to the microsporidium treated herein, but ultrastructural differences (e.g. a shorter polar filament without a constriction) and the different host (mites of the genus *Limnochares*) reveal distinctly that these species are different. It can therefore be concluded that the species described herein differs both from the *Napamichum* species and from microsporidia of midges with similar sporogony.

The genus *Napamichum* conforms with many genera of *The-*

←

the distinct delimitation towards the endospore, and no. 5 indicates the double-layer. The two arrows indicate the envelopes of two adjacent sporophorous vesicles; the electron dense material between the vesicles is the host cell cytoplasm. Bar = 50 μm. **19**. Electron micrograph of a row of transversely sectioned polar filament coils, the first four coils exhibit 5 distinct layers (I–V); the same layers can be distinguished in the last three coils, although they are not quite mature. Bar = 50 nm. Fig. 15–16: Heidenhain's haematoxylin.

Table 1. Octosporous microsporidia with oval-pyriform shaped spores isolated from midge larvae. (F = fresh smears, S = fixed and stained smears.)

Species References	Spores, shape and dimensions in smears (μm)	Sporophorous vesicles, shape and dimension in smears (μm)	Tissues affected	Host Country
Amblyospora macrococcus (Voronin, 1979)	Barrel-shaped 4.5–5.2 × 6.0–6.7 F 3.8–4.5 × 4.8–5.5 S	Circular 15–17	Fat body	*Corynoneura* sp. Russia
Amblyospora sp. Voronin, 1991	Barrel-shaped —	— —	Fat body	*Cricotopus ex gr. silvestris* Russia
Amblyospora sp. Garcia & Lange, 1986	Barrel-shaped 2.4–2.7 × 2.9–3.7 S	— —	Fat body	*Eukiefferiella* sp. Argentina
Thelohania breindli Weiser, 1946	Oval 1 × 2–3 S	Circular —	Fat body	*Chironomus thummi* Czechoslovakia
Thelohania corynoneurae Voronin, 1979	Oval, one end pointed 2.9–3.6 × 4.4–5.4 S 3.1–3.7 × 5.3–6.4 F	Circular —	Fat body	*Corynoneura* sp. Russia
Thelohania pinguis Hesse, 1903	Oval (-pyriform) 2 × 3–3.5	Circular 6–6.5 Ellipsoid 4 × 7	Fat body	*Tanypus varius* France
Thelohania sp. Hilsenhoff & Lovett, 1966	Pyriform 1.8–2.0 × 3.4–3.8	Circular-oval —	Fat body	*Chironomus plumosus* USA
Napamichum dispersus (Larsson, 1984)	Pyriform 2.5–2.8 × 3.7–5.5 S −3.5 × −6.0 F	Fusiform 4–6 × 10–14 S	Fat body	*Endochironomus* sp. Sweden
N. cellatum n. sp. hoc loco	Pyriform 2.1–2.4 × 3.7–4.5 S	± Fusiform 11.7–14.3 × 13.8–17 S	Fat body	*Endochironomus* sp. Sweden

lohania-like microsporidia when only the light microscopic aspect is considered [4]. The discriminating characters were mostly taken from the ultrastructural cytology: the layers of the exospore, the anisofilar polar filament, the construction of the two parts of the polaroplast, and the inclusions of the episporontal space [6]. Comparing the new species with the other two species of the genus, the similarities are obvious, further justifying the establishment of the genus *Napamichum*. Also, this species conforms in detail with the layering of the exospore, the layering of the polar filament and the construction of the polaroplast. However, even if all three species have the three kinds of inclusions of the episporontal space (granules or fibres, crystals composed of material of two densities, and tubules), there are minor differences concerning details. The prominent fibres are unique to *N. aequifilum* (see Fig. 4a in [6]) while in *N. dispersus* (Fig. 26 in [5]) and the new species (Fig. 20) the material appears granular. A similar difference is seen in the crystals: *N. aequifilum* has dense material in the centre (Fig. 4B in [6]), while *N. dispersus* (Fig. 26 in [5]) and the species treated herein (Fig. 21) have the dense material in the external zone. In addition the crystals of *N. dispersus* are associated with zones of amorphous material. The distinct honeycomb- or network-like aggregates, seen at the time the crystals are formed, are unique to the new *Napamichum* species.

Napamichum cellatum sp. nov. (Fig. 1–23)

Merogony. As for the genus. Plurinucleate plasmodia probably divide by plasmotomy. Merozoites measure 2.8–3.7 μm, and their diplokarya measure 1.6–2.6 μm in diameter.

Sporogony. As for the genus. Abnormal sporogony resulting in multisporoblastic sporophorous vesicles with partly anomalous sporoblasts were observed.

Spores. Slightly pyriform. Dimensions of fixed and stained spores: 2.1–2.4 × 3.7–4.5 μm. Spore wall 168–242 nm thick; exospore five-layered, 50–57 nm. Polar filament anisofilar with seven to eight coils (4–5 + 3–4), 142–156 and 120 nm in diameter; five distinct layers visible in the transversely sectioned filament. The angle of tilt is 55–65°. The anterior lamellar part of the polaroplast extends backwards for about ¼ of the spore length. Posterior polaroplast section with membrane-bound, tubular-like compartments. Polar sac encloses the anterior ⅔ of the anterior polaroplast region. Nucleus up to 0.9 μm in diameter, in the midsection of the spore. Vacuole, 1.0–1.1 μm in diameter, at the posterior end of the spore.

Sporophorous vesicle. A membraneous envelope, approximately 6 nm thick, encloses the microsporidium from the beginning of sporogony. Finely granular, crystal-like and tubular inclusions of exospore wall origin appear and disappear during the sporogony. Vesicles with mature spores have only traces of inclusions. Crystal-like inclusions are prominent using haematoxylin staining and nearly invisible in Giemsa stainings.

Type host. Larva of *Endochironomus* sp. (Diptera, Chironomidae).

Host tissues involved. The fat body, including slight hypertrophy.

Type locality. Small pond, near the village of Vikhög, Scania, Sweden.

Types. Holotype on slide No. 861007-C-4, paratypes on slides No. 861007-C-1–8.

Deposition of types. The slide with the holotype was deposited in the International Protozoan Type Slide Collection at Smithsonian Institution, Washington, DC (USNM #43215), paratypes in the collection of Dr. J. Weiser, Charles University, Prague, Czech Republic, and in the collection of the senior author (USNM #43216).

Etymology. The species name *cellatum* alludes to the honeycomb-like inclusions present around the lobed sporogonial plasmodium.

ACKNOWLEDGMENTS

We wish to thank Ms. Lina Gefors, Ms. Birgitta Klefbohm, and Ms. Inger Norling, Department of Zoology, University of Lund, and Ms. Agneta Persson, Department of Anatomy, University of Lund, for skilful technical assistance. We are also greatly indebted to Fil. mag. Vera Ulver for translations of Czech

and Russian manuscripts, and to the staff of the Electron Microscopy Unit of the Departments of Medicine, Lund. The investigation was financially supported by grants from the Royal Swedish Academy of Sciences and the Swedish National Science Research Council.

LITERATURE CITED

1. Garcia, J. J. & Lange, C. E. 1986 [publ. 1987]. Contribucion al conocimiento de los microsporidios argentinos. I. *Amblyospora* sp. (Microsporida, Thelohaniidae) en *Eukiefferiella* sp. (Diptera, Chironomidae). *Neotropica (La Plata)*, **32**:61–65.

2. Hesse, E. 1903. Sur la présence de Microsporidies du genre *Thelohania* chez les Insectes. *C. R. Acad. Sci. Paris*, **137**:418–419.

3. Hilsenhoff, W. & Lovett, O. L. 1966. Infection of *Chironomus plumosus* (Diptera: Chironomidae) by a microsporidian (*Thelohania* sp.) in Lake Winnebago, Wisconsin. *J. Invertebr. Pathol.*, **8**:512–519.

4. Hazard, E. I. & Oldacre, S. W. 1975. Revision of Microsporida (Protozoa) close to *Thelohania*, with descriptions of one new family, eight new genera and thirteen new species. *U.S. Dep. Agric. Techn. Bull.* No. 1530. Pp. 1–104.

5. Larsson, J. I. R. 1984. Ultrastructural study and description of *Chapmanium dispersus* n. sp. (Microspora, Thelohaniidae), a microsporidian parasite of *Endochironomus* larvae (Diptera: Chironomidae). *Protistologica*, **20**:547–563.

6. Larsson, J. I. R. 1990. Description of a new microsporidium of the water mite *Limnochares aquatica* and establishment of the new genus *Napamichum* (Microspora, Thelohaniidae). *J. Invertebr. Pathol.*, **55**:152–161.

7. Reynolds, E. S. 1963. The use of lead citrate at high pH as an electron-opaque stain in electron microscopy. *J. Cell Biol.*, **17**:208–212.

8. Romeis, B. 1968. Mikroskopische Technik. Oldenbourg Verlag, München, Germany.

9. Voronin, V. N. 1979. New species of microsporidia (Protozoa) from larvae of *Corynoneura* (Diptera, Chironomidae). *Zool. zhurnal* (Moscow), **4**:592–594. (Russian with English summary.)

10. Voronin, V. N. 1991. The ultrastructure of two microsporidian species of the genus *Amblyospora* (Microsporidia: Amblyosporidae) from the midge larvae (Diptera: Chironomidae). *Tsitologia* (St. Petersburg), **10**:67–74. (Russian with English summary.)

11. Weiser, J. 1946. The microsporidia from chironomid larvae. *Vestn. Cs. spol. zool.*, **10**:273–292. (Czech with English summary.)

Received 12-2-93, 2-18-94; accepted 3-15-94

J. Euk. Microbiol., 41(5), 1994, pp. 457–463

Evidence for the Ancestral Origin of Group I Introns in the SSUrDNA of *Naegleria* spp.

JOHAN F. DE JONCKHEERE

Protozoology Laboratory, Department of Microbiology, Institute of Hygiene and Epidemiology, J. Wytsmanstraat 14, B1050 Brussel, Belgium

ABSTRACT. The sequence variation within the group I intron in five *Naegleria* spp. was studied and compared with the sequence variation within the flanking small subunit ribosomal DNA. Considerable sequence divergence was observed in the introns as well as in the rDNA. In the intron deletions and insertions are only detected in the sequence contributing to the secondary structure, not in the open reading frame. Most of the sequence variation is detected in the unpaired loops. In the case of nucleotide substitution in helices, compensating base pair changes were observed. The sequence variation does not induce variation in the secondary structure model. The phylogenetic tree based on the intron sequences is similar to the tree based on the flanking rDNA sequences. This observation indicates that the intron might have been acquired at an early stage in evolution, and lost in the majority of *Naegleria* spp.

Supplementary key words. Open reading frame, phylogenetic tree, secondary structure.

NAEGLERIA fowleri is an amoebo-flagellate that infects the human brain causing death within a week [1]. Only one other free-living *Naegleria* sp., *N. gruberi*, was known when this pathogen was described. Searches for *N. fowleri* in the environment have been performed all over the world. Many of the strains isolated did not fall within the variability of the 2 known species, and new species and subspecies were created. In a recent revision of the *Naegleria* taxa based on small subunit ribosomal DNA (SSUrDNA) sequencing [7], the subspecies were elevated to species rank. A total of 10 species are now accepted, while more species will probably be defined in the future [21]. In 5 *Naegleria* spp. a group I intron was found in helix 19 of the SSUrDNA [5]. All strains belonging to these species, whatever their geographic origin, harbor the intron. The use of restriction enzymes has already indicated that the intron differed in sequence according to the *Naegleria* sp. [6]. The intron sequences for the different *Naegleria* spp. are reported here and the phylogenetic relationships between the introns are compared with the phylogenetic relationships between the *Naegleria* spp. based on the SSUrDNA sequences flanking the intron.

MATERIALS AND METHODS

The SSUrDNA was amplified using the polymerase chain reaction (PCR) with the 5′-end-specific primer TACCTGGTTGATCCTGACCAG and the 3′-end-specific primer AAATGATCCCTACGCAGGTT based on the 18S rDNA sequence published for *N. gruberi* [3]. All *Naegleria* spp. have 2 conserved Pst I sites in the SSUrDNA and a group I intron is present between these two Pst I sites in *N. andersoni, N. jamiesoni, N. italica, N. italica* related strains and one cluster of *N. gruberi* [5]. The *N. italica* related strain has since been named *N. clarki* [7]. The strains used in this study are from my own collection and are A-2, T56E, AB-T-F3, RU30 and CCAP 1518/1D, respectively. The Pst I fragment containing the group I intron in one strain of these species was ligated into the plasmid pUC18. Nested deletions were produced with the Exo III/S1 technique using the Erase-a-Base kit (Promega, Madison, WI). The sequencing was performed using the dideoxynucleotide chain termination method with modified T7 DNA polymerase using the Sequenase (version 2.0) kit and protocol from the US Biochemical Corporation (Cleveland, OH) and [^{32}P] α-dATP. In addition to dGTP, dITP was included to eliminate compressions due to secondary structures. In the deletion clones of *N. italica*, DNA rearrangements were observed. Therefore, *N. italica* and *N. clarki* were sequenced with the Δ Taq cycle sequencing kit (US Biochemical Corporation, Cleveland, OH) using primers complementary to rDNA flanking the intron in stem 19 (5′ end specific: CATTGGAGGAAAAGTCTGGT 3′ end specific: